

Surfactant-free synthesis of metallic bismuth spheres by microwave-assisted solvothermal approach as a function of the power level

Miriam ESTRADA FLORES (✉)^{1,2,3}, Patricia SANTIAGO JACINTO², Carmen M. REZA SAN GERMÁN³, Luis RENDÓN VÁZQUEZ², Raúl BORJA URBY⁴, and Nicolás CAYETANO CASTRO⁴

1 Instituto de Investigaciones en Materiales, Circuito Exterior S/N, Zona de Institutos, Ciudad Universitaria, C.P. 04510, México, D.F., México

2 Instituto de Física, Circuito de la Investigación Científica, Edificio Marcos Moshinsky, Laboratorio de Materiales Nanoestructurados, Ciudad Universitaria, C.P. 04510, México, D.F., México

3 Escuela Superior de Ingeniería Química e Industrias Extractivas, Unidad Profesional Adolfo López Mateos Edif. Z-5 2do. Piso, Instituto Politécnico Nacional C.P. 07738, México, D.F., México

4 Centro de Nanociencias y Micro y Nanotecnologías. Instituto Politécnico Nacional, Av. Luis Enrique Erro S/N, Unidad Profesional Adolfo López Mateos, Zacatenco, Delegación Gustavo A. Madero, C.P. 07738, México, D.F., México

© Higher Education Press and Springer-Verlag Berlin Heidelberg 2016

ABSTRACT: In the present work, the synthesis of micro- and nano-sized spheres of metallic bismuth by microwave-assisted solvothermal method is reported. The synthesis method was carried out at different power levels and at a unique frequency of microwave irradiation. The sphere sizes were controlled by the microwave power level and the concentration of dissolved precursor. Structural and morphological characterization was performed by SEM, HRTEM, EELS and XRD. The results demonstrated that rhombohedral zero valent Bi spheres were synthesized after microwave radiation at 600 and 1200 W. However, if the power level is decreased to 120 W, a monoclinic phase of Bi₂O₃ is obtained with a flake-like morphology. In comparison with a conventional hydrothermal process, the microwave-assisted solvothermal approach provides many advantages such as shorter reaction time, optimum manipulation of morphologies and provides a specific chemical phase and avoids the mixture of structural phases and morphologies which is essential for further applications such as drug delivery or functionalization with organic materials, thanks to its biocompatibility.

KEYWORDS: microwave oven; power level; metallic bismuth; spherical structures; mechanism of formation; electron energy loss spectroscopy (EELS)

Contents

- 1 Introduction
- 2 Materials and methods
- 3 Results and discussion
 - 3.1 Experimental results
 - 3.2 The reduction mechanism
 - 3.2.1 The starting stage
 - 3.2.2 The reduction mechanism from Bi⁵⁺ to Bi³⁺
 - 3.2.3 The reduction mechanism from Bi³⁺ to Bi⁰

4 Conclusions

Acknowledgements

References

Received July 1, 2016; accepted August 30, 2016

E-mail: mestrada@fisica.unam.mx

1 Introduction

A synthesis by microwave-assisted solvothermal is employed to generate materials with different morphologies. Bismuth structures as spheres [1–4], flakes [5], rods [6] and hollow spheres [7] have been synthesized by this method. Microwave-assisted solvothermal is widely used in the synthesis of micro- and nano-structured materials [8–13] because of being a readily available technique capable of minimizing the time required for the production of different structures and morphologies because its heating rate is different than conventional heating as mentioned by Knochel and Molander [14]. Significant rate-accelerations have been observed when the microwave-assisted solvothermal protocol was compared with the conventional thermal method. For example, Kappe [15] reduced the reaction times from 12–48 h with conventional heating at 80°C to 5–15 min with microwave flash heating at 200°C in different organic solvents.

Solvothermal approach with conventional heating uses conduction and convection processes to increase the temperature of a system, while microwave heating employs electromagnetic fields. Microwaves correspond to a section of the electromagnetic spectrum with frequencies in the range of 0.3–300 GHz. The corresponding wavelengths of these frequencies are from 1 m to 1 mm. The most commonly used frequency is 2.45 GHz, which corresponds to a wavelength of 12.3 cm. The interaction of microwaves with a dielectric medium is related to the material's dielectric constant as Sutton demonstrated in his research [16]. When a material is polarized in an alternating field some energy is lost as heat. The microwaves can also be able to initiate chemical reactions not possible in conventional processing through selective heating of reactants as well as new materials may be created [17]. The microwave radiation interacts directly with the molecules in the reaction mixture, leading to a sudden rise in temperature. A chemical reaction cannot be generated from the direct interaction of the electromagnetic energy and precursor materials. However, the ability of a specific material to convert the energy from microwaves to heat determines the efficiency of dielectric heating [18]. Ethylene glycol is one of the most employed dissolvents in synthesis by microwave due to its high absorption behavior and swift heating (loss tangent of 1.350). The heating mechanism by microwave is generated by the vibration of molecules. These molecules are excited with low energy waves that do not break bonds of molecules themselves. However, the

dissolvent is a very important factor to increase the temperature inside the digestion vessel. When the activation energy of the reactants is higher than the necessary to break the bonds of inorganic molecules inside the vessel, the reduction process begins. The electric component of a magnetic field generates heating by two mechanisms, which consist of dipolar polarization where the rotational motions of polar molecules result from aligning the dipoles of the molecules with the alternating electric fields of the microwave radiation and ionic conduction when ions move through a solution under the influence of an electric field. Energy loss occurs through high speed collisions, which result in the conversion of kinetic energy into heat [19–22].

Metallic bismuth has interesting properties, such as diamagnetism and high temperature superconductivity. Currently, metallic bismuth is employed in several medical applications to treat a variety of medical disorders. Also, it is commonly employed as a drug transport medium within the human body. Bismuth owes its versatility to its crystalline structure. Likewise, it typically contains a large number of vacancies, which makes it a material capable of growing with different morphologies and phases [23–25]. Metallic bismuth is also a promising candidate for composite materials such as Bi_2Te_3 [26–27], BiSbTe [28], or Bi_2Se_3 [29] (e.g., thermoelectric elements). Bismuth oxide is widely used as a component of sensors, solar cells, glasses and architectural sealants due to its durability and stability. Moreover, applications in optical devices and superconductors have been found [30]. Compounds that are based on bismuth oxide have been employed in mapping images that involve X-rays [31], as well as having been reported in studies of photocatalytic [32–33] and oxidation-catalyzed reactions [34–35].

Noble metal nanoparticles are a highly promising class of nanomaterials for novel biomedical applications due to their general lack of toxicity [36]. These applications suggest that metallic bismuth could be used for drug delivery because of its biocompatibility [37–41]. Spheres of metallic bismuth functionalized with proteins can be exceptional devices for drug delivery to cure specific diseases. Therefore, this material could be inserted into the human body, where the proteins are released and the biocompatible dose of bismuth spheres are expelled by natural human processes. Medical approaches have been reported in the study of interaction of TiO_2 with dopamine [42].

In the present work, the syntheses of micro- and nano-sized spheres of metallic bismuth are reported by

microwave-assisted solvothermal approach. The synthesis method was carried out at different power levels and at a unique frequency of microwave irradiation. The sphere sizes were controlled by the microwave power level and the concentration of dissolved precursor. The power level of the microwave is an important factor to determine the phase and morphology of materials obtained from the synthesis of sodium bismuthate and ethylene glycol. The synthesis at higher power level (600 and 1200 W) generates spheres of metallic bismuth. However, at a lower level, such as 120 W, the product obtained is Bi_2O_3 with a flake-like morphology. The specific characteristics of spherical metallic bismuth and flake-like bismuth oxide were controlled by two variables: the concentration of the dissolved precursor and the microwave power level. The potentiality of this work resides in the fact that we found the conditions to produce zero valent spheres of bismuth phase under specific variables and understood the reduction process mechanism of the synthesized materials. Additionally, this procedure provides a specific chemical phase and morphology and avoids the mixture of structural phases and morphologies which are essential for further applications such as drug delivery or functionalization with organic materials.

2 Materials and methods

A microwave-assisted solvothermal synthesis was employed. A series of three concentrations of precursor solutions were employed in a range from 0.01 to 0.05 mol/L.

Solutions of BiNaO_3 at 0.01, 0.03 and 0.05 mol/L were prepared using ethylene glycol (J.T. Baker) as a solvent and reagent grade sodium bismuthate (Sigma-Aldrich). The samples were stirred for half an hour at room temperature. The corresponding sample of 0.05 mol/L was a super-saturated solution. These solutions were poured into a Parr acid digestion vessel model 4781 with a capacity of 23 mL. The vessel was introduced into a microwave, Panasonic model NE-1258R. The microwave frequency was synthesized at 2.45 GHz. It was used with three different power levels: 1200, 600 and 120 W for 3 min per sample. The experimental conditions are shown in Table 1.

After irradiation, the samples were cooled at room temperature. Then, they were washed several times with distilled water and ethyl alcohol. The products obtained were dried at 70°C for 1 h to eliminate residual ethyl alcohol. The samples synthesized at 1200 and 600 W at all concentrations were grey, while the samples corresponding

Table 1 Experimental conditions

Microwave power level /W	Precursor concentration /($\text{mol}\cdot\text{L}^{-1}$)		
120	0.01	0.03	0.05
600	0.01	0.03	0.05
1200	0.01	0.03	0.05

to the synthesis at 120 W were a light sand color, suggesting the presence of a bismuth oxide phase.

The results of the sample analysis allowed us to understand the influence of each one of the variables in the microwave-assisted solvothermal method. This information allowed us to divide the results in two parts: high power level (600 and 1200 W) and low power level (120 W). We emphasize the results of the samples obtained at high power level because these predominantly generated spherical metallic bismuth systems.

Samples were characterized by X-ray diffraction (XRD) to determinate the crystalline phases; a Rigaku diffractometer model Miniflex 600 with Cu $K\alpha$ radiation ($\lambda = 1.54 \text{ \AA}$), a lineal focus, 40 kV and 15 mA was used. A Soller Ni 0.5-mm slit filter was placed in the incident beam. Measurements were performed with a scanning geometry of 3° to 100° using a step size of 0.01° and a rate of 3(°)/min.

A JEOL JSM-5900LV SEM equipped with energy dispersive spectroscopy (EDS) was employed to identify the morphology and size of the spheres.

High-resolution transmission electron microscopy (HRTEM) was performed on a JEOL JEM-ARM2006F to determine the crystalline properties of the nanospheres. Electron energy loss spectroscopy (EELS) was made for the samples synthesized at high power level in order to discriminate between the plasmon of metallic Bi and the corresponding bonding of bismuth oxide.

3 Results and discussion

3.1 Experimental results

This study is focused on the control of a predominant chemical phase with a single morphology avoiding the mixture of structures in order to provide a specific phase to get a better control for further design of functionalized materials. Therefore, characterizations of the high power synthesis, which formed spheres of metallic bismuth, are shown first. Finally, we report the results obtained from growth at a low power level, which formed flake-like structures of bismuth oxide.

The XRD results show structures of a single crystalline

phase in the samples synthesized at powers of 600 and 1200 W. All the samples obtained at high power level of microwave are composed of metallic bismuth for all concentrations of the precursor solution, in agreement with PDF Card # 44-1246. These samples belong to the rhombohedral system with space group Rm (166), with cell parameters of $a = 4.547 \text{ \AA}$ and $c = 11.861 \text{ \AA}$. The strongest intensity diffraction peaks correspond to the $\{012\}$ family planes. They also show two characteristic planes of growth for metallic bismuth: (104) and (110).

The SEM analysis revealed the morphology of the product obtained for each set of experimental conditions. With 600 and 1200 W, a spherical morphology is observed and the variation in each case is just the size of the spheres as it is shown in the histograms.

In a deeper analysis, the samples obtained at a microwave irradiation of 600 W show diffraction patterns with sharp peaks that indicate the formation of crystalline Bi microstructures (Fig. 1). At 0.01 mol/L spherical structures smaller than $1 \mu\text{m}$ were found (Fig. 2(a)) typically in the range of 500–600 nm (Fig. 2(b)). At a higher magnification, HRTEM indicates that the matrix is composed of bismuth nanoparticles with an average size of 5 nm. The nanoparticles are surrounded by residues of the precursor. When the concentration of the precursor solution is increased to 0.03 mol/L, the sample presented an assembly of individual spheres, with sizes from 600 to 700 nm (Fig. 2(d)). Because of this, it is evident that the residual precursor salt was essentially reduced (Fig. 2(c)). An additional sample was synthesized at a concentration of 0.05 mol/L. The production of large and isolated spheres (Fig. 2(e)) with 700–800 nm in diameter (Fig. 2(f)) is a consequence of a higher solute concentration.

The microwave-assisted solvothermal synthesis offers a swift crystallization because it generates a uniform heating of the reaction mixture with the creation of hot spots. The rapid heating and creation of hot spots are important factors associated with an increase in synthesis rates. Under microwave irradiation, the stage of synthesis between nucleation and crystal growth is accelerated. At high power level, the photon number increases and the precursor solution is reduced to metallic bismuth. The hot spots are generated uniformly on the precursor solution and the nucleation process begins. The sudden heating promotes the growth of crystal and the sphere is enlarged. In conclusion, for 600 W, the concentration has an evident influence on the size of the spheres. At higher concentration, the spheres grow with a major size.

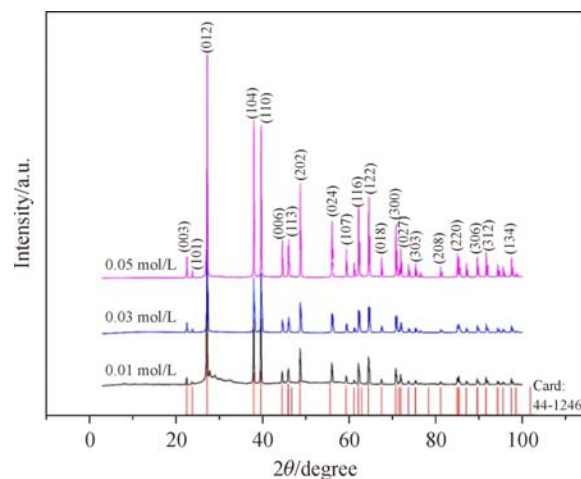


Fig. 1 XRD patterns of metallic bismuth samples that were obtained under different concentrations of the precursor solution and irradiated at 600 W.

The XRD patterns from samples obtained at 1200 W (Fig. 3) show sharp peaks that suggest large crystalline structures of metallic Bi. In this case, individual spheres are formed too, but the size is in the order of microns. A sample synthesized at a concentration of 0.01 mol/L displays spheres that are between 3 and $5 \mu\text{m}$ (Figs. 4(a) and 4(b)). At a higher concentration of precursor solution (0.03 mol/L), the sphere sizes decreased to 1–3 μm (Figs. 4(c) and 4(d)). At 0.05 mol/L we obtained the smallest spheres for this particular power level, with sizes less than $1 \mu\text{m}$ (Figs. 4(e) and 4(f)). In conclusion, when the concentration behavior is at 600 W, the size of the spheres decreases in contrast to the time when the concentration is at a higher power level (1200 W), indicating that if we use a higher microwave power, the temperature of the system is increased and generates a smaller average sphere size with a saturated solution.

At higher power level, a superheating of the solution is generated; the pressure of the vessel is increased. The nucleation and crystal growth begins and produces spheres in the order of $5 \mu\text{m}$ size at low concentration of the reactant. When the concentration is increased to 0.03 mol/L, smaller spheres are synthesized because the pressure of the vessel is higher when the amount of the reactant is raised. Moreover, if the concentration is modified to 0.05 mol/L we can observe that the average size of the spheres is in the order of $1 \mu\text{m}$ or less. In conclusion, the size of the spheres depends on the concentration of the precursor solution and consequently, on the pressure reached in the vessel.

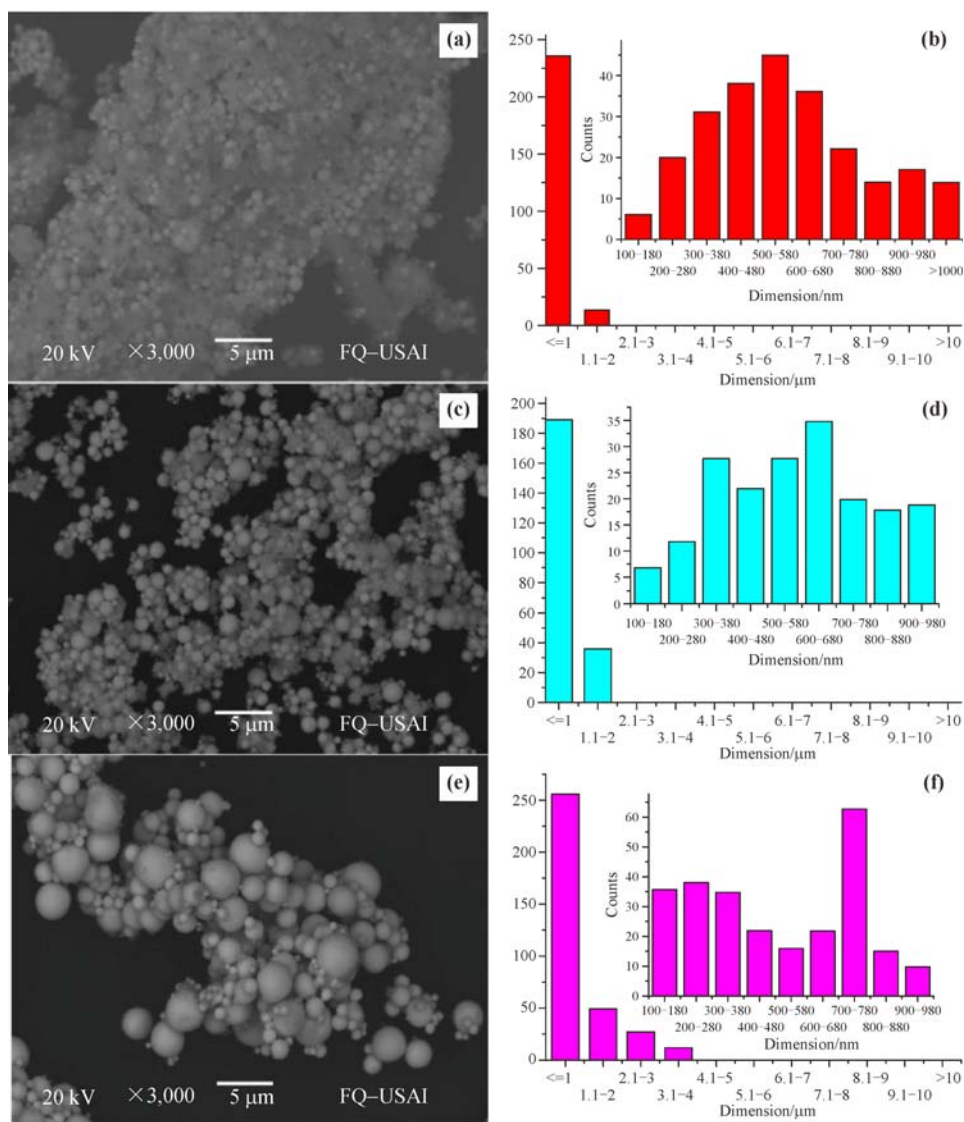


Fig. 2 SEM images of metallic bismuth synthesized at 600 W, with the precursor concentrations of (a) 0.01 mol/L, (c) 0.03 mol/L and (e) 0.05 mol/L, and histograms of the sphere sizes corresponding to (b) 0.01 mol/L, (d) 0.03 mol/L and (f) 0.05 mol/L.

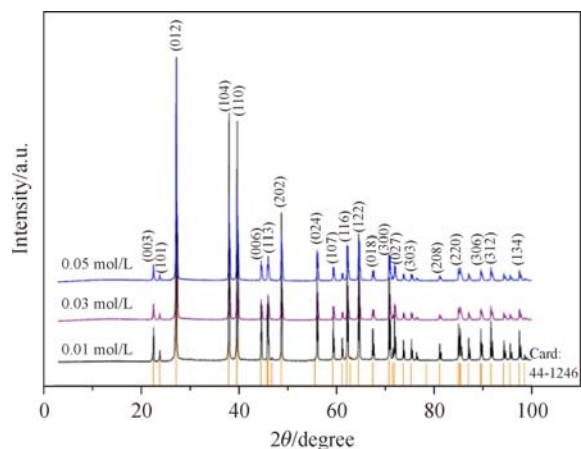


Fig. 3 XRD patterns of metallic bismuth samples obtained with different concentrations of precursor solution at 1200 W of irradiation of microwave.

In addition, at microwave power level of 600 and 1200 W, the products belonged to a single phase of metallic bismuth due to the complete reduction of Bi^{5+} to metallic Bi.

The sample with small individual spheres (600 W and 0.03 mol/L) was further characterized by HRTEM to measure the distance between lattice fringes and to determine the main crystallographic phase.

HRTEM images show bismuth nanoparticles in the range of 5–15 nm (Fig. 5(a)). These particles represent the initial stage in the growth mechanism of metallic bismuth spheres that are shown in Fig. 5(b). This hypothesis is based on the evidence that consists in the nanoparticles being made of metallic bismuth. This result is confirmed by the XRD patterns that show the lattice distances which correspond with PCPDF Card: 44-1246.

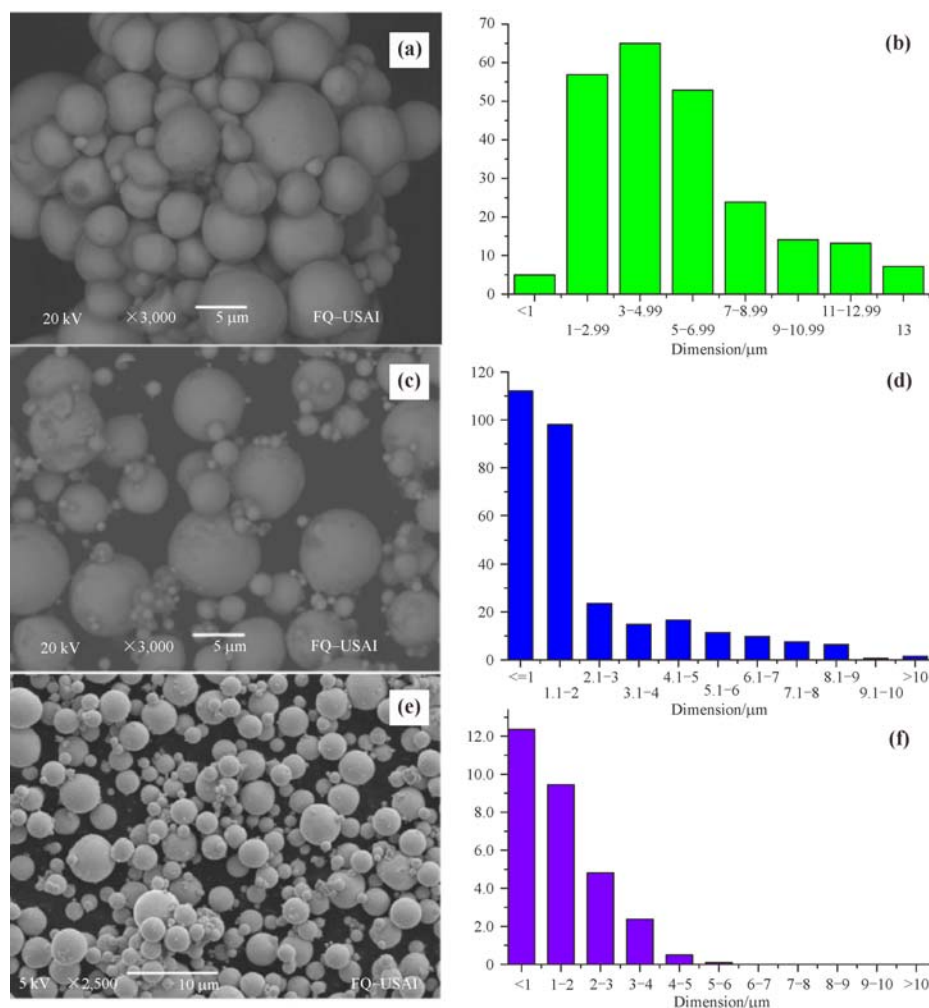


Fig. 4 SEM images of metallic bismuth synthesized at 1200 W with the precursor concentrations of (a) 0.01 mol/L, (c) 0.03 mol/L and (e) 0.05 mol/L, and histograms of their respective images corresponding to (b) 0.01 mol/L, (d) 0.03 mol/L and (f) 0.05 mol/L.

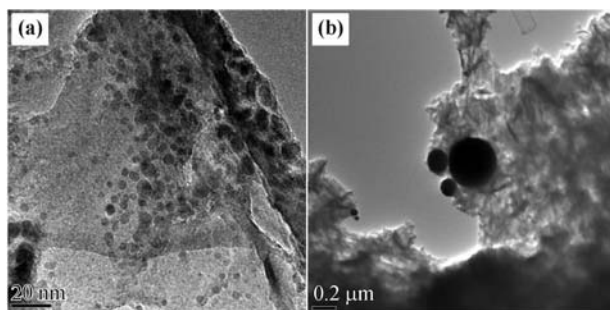


Fig. 5 (a) HRTEM image of metallic bismuth nanoparticles embedded in a matrix of residual reactant. (b) Low magnification micrograph of bismuth spheres in the order of 200–500 nm.

The lattice fringes of metallic bismuth were found by the HRTEM analysis. Figure 6 shows the principal lattice distances associated with the growth directions of the metallic bismuth. The data displayed in Fig. 6 agrees with

PDF Card 44-1246. The lattice fringe distance of 3.3 Å belongs to the (012) plane, while 2.03 Å corresponds to the reflection of {015} family planes (Fig. 6(a)); the (014) plane matches with an interplanar distance of 2.4 Å (Fig. 6(b)); the (110) plane presents an interplanar distance of 2.27 Å (Fig. 6(c)). All of this information is consistent with rhombohedral bismuth reflections. HRTEM images show zones of polycrystalline Bi.

The experimental EELS spectrum was obtained at 200 keV with a GIF Quantum Energy Filter. The spectrum shows the transition of the bismuth element in the energy loss region of 440 eV and the absence of oxygen transition at K edge.

The EELS spectrum was obtained from a thin zone of a polycrystalline sphere synthesized at 600 W (Fig. 7). The spectrum shows a N45 absorption edge due to transitions of 4d electrons into unoccupied states of the partially filled 4f

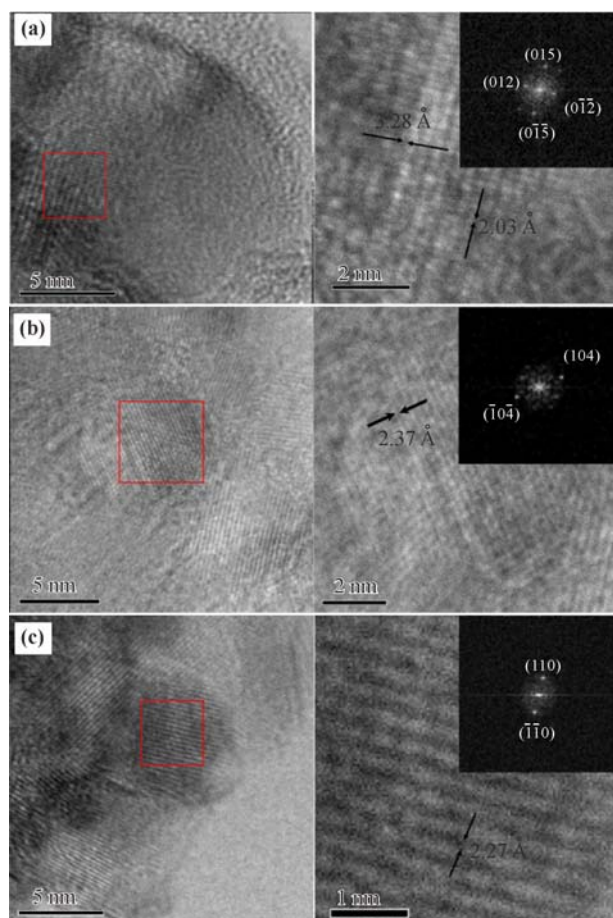


Fig. 6 HRTEM images of metallic bismuth synthesized at 600 W and 0.03 mol/L, with the interplanar distances given for (a) (012) and (015), (b) (104), and (c) (110) planes.

shell. Around this zone, at 532 eV we should have found the K edge of oxygen. However, from our experimental spectra we can assure that the particles correspond to the metallic bismuth phase instead of bismuth oxide.

At lower microwave power level (120 W), the microwave-assisted solvothermal system does not get enough production of carbocations to break the bonds between Bi and O. XRD patterns of the samples produced from 0.01 mol/L to 0.05 mol/L solution are shown in Fig. 8(a). The result is the formation of bismuth hydroxide from the concentration of 0.01 mol/L and Bi_2O_3 to concentrations of 0.03 and 0.05 mol/L. In this case, the reduction of Bi^{5+} was incomplete and did not yield zero valent Bi, as shown at higher power conditions.

Samples synthesized at low microwave power level (120 W) and concentration solution of 0.01 mol/L produce bismuth hydroxide, which agrees with the information obtained from PDF Card # 01-001-0898. In this case, the

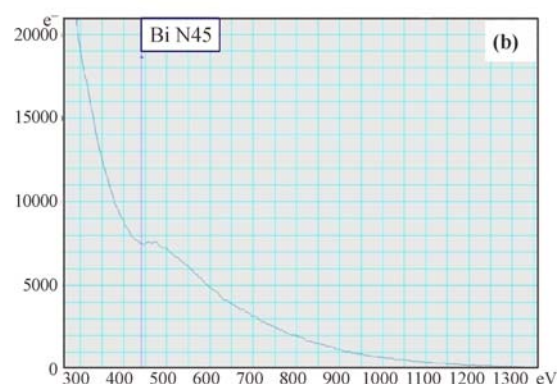
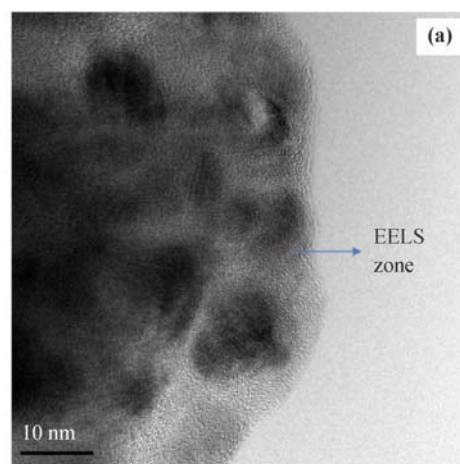


Fig. 7 (a) A sphere thin zone of the sample obtained at 600 W. (b) The corresponding EELS spectra showing the N45 absorption edge at 440 eV.

bismuth hydroxide is obtained because the bismuth oxide is not dehydrated with help of the medium. For these experimental conditions, micro-flake morphology with an average size of 5 μm was obtained as it is shown in Fig. 8(b).

At the same power level and precursor solution concentrations of 0.03 and 0.05 mol/L bismuth oxides are produced because Bi^{5+} is reduced to Bi^{3+} . Those samples were consistent with the information obtained from PDF Card # 01-079-6670 and belong to the monoclinic crystal system with space group $\text{P}2_1/\text{c}$. At a concentration of 0.03 mol/L, flower-like structures growing out from the micro-flakes were observed (Fig. 8(c)). In this case, the precursor was completely dissolved to allow the growth in flower-like structures. At 0.05 mol/L, the dissolution of the precursor salt creates a supersaturated solution that generates agglomerated structures larger than 10 μm formed by flakes as it is possible to observe in Fig. 8(d).

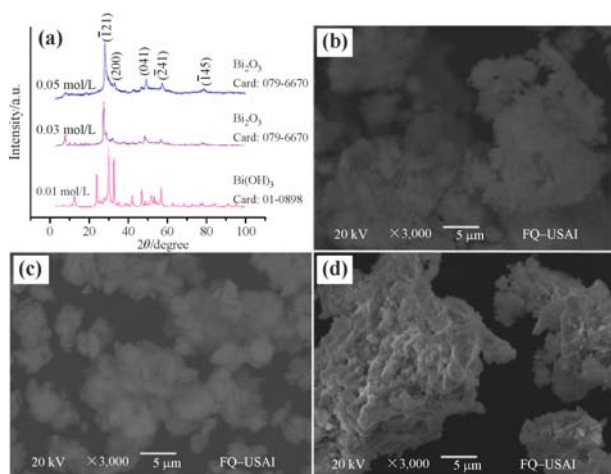


Fig. 8 (a) XRD patterns of samples obtained at 120 W with different concentrations. SEM images of (c) 0.03 mol/L and (d) 0.05 mol/L which correspond to a Bi_2O_3 and (b) Bi(OH)_3 structures which correspond to 0.01 mol/L.

3.2 The reduction mechanism

The results obtained by the previous techniques allow us to suggest a mechanism for the reductions of metallic bismuth and bismuth oxide.

The reduction mechanism starts with the interaction of the microwaves with ethylene glycol solvent. In the second stage, the precursor solution of sodium bismuthate contains Bi^{5+} ions that are reduced to Bi^{3+} . In the last stage of this process, metallic bismuth is obtained after the complete reduction of Bi^{3+} to Bi^0 .

3.2.1 The starting stage

The reaction begins with the interaction between photons from the microwave oven and ethylene glycol generating the carbocations and water subproducts. To start the reaction, some bonds must be broken, which requires ions for this propose. The most reactive molecules are the organic ones, because they need lower activation energy to break the bonds. When microwaves interact with ethylene glycol, a carbocation is formed due to the dehydration of the reactant. This mechanism is shown in Fig. 9.

3.2.2 The reduction mechanism from Bi^{5+} to Bi^{3+}

Bismuth oxide is the result of the reduction from Bi^{5+} to

Bi^{3+} . This process takes place in the second stage of the synthesis. The reactive carbocation attempts to stabilize itself with the help of BiO_3 carbanion from NaBiO_3 of the precursor solution. At high alkaline pH, bismuth hydroxide is produced, and its dehydration generates bismuth oxide [43–44]. In this case, the reaction mechanism is as shown in Fig. 10.

3.2.3 The reduction mechanism from Bi^{3+} to Bi^0

In the third stage of the synthesis, to yield metallic Bi, the reduction process of Bi^{3+} to Bi^0 is carried out. Hydronium ions form hydrogenated structures rearrange themselves to form water molecules, acetic acid, and metallic bismuth. The pH value decreases after the reaction. Then, the formation of an acid product is justified. XRD shows a single Bi phase without bismuth oxides. This suggests a reaction mechanism for the synthesis of metallic bismuth shown in Fig. 11 [45].

When the power level is increased, the number of photons of the system also increases, and there are more photons to produce carbocations to begin the reduction process of the sodium bismuthate in the ethylene glycol. The microwave-assisted solvothermal synthesis also generates hot spots and a superheating of the reactant solution which begins with the nucleation and crystal growth. The process begins at 600 W with the nucleation of metallic bismuth where an increase of the size spheres is observed as a function of the concentration of the precursor solution. However, at higher power level (1200 W), the temperature of the solution in the vessel is higher, and the pressure inside the container is increased too. The pressure is also modified by the concentration of the solution. At higher concentration of the reactant the pressure of the vessel increases. These experimental conditions inhibit the crystal growth process. Then, supersaturated solutions at 1200 W produce smaller spheres than those produced at a lower power level with a supersaturated solution.

At very low power level such as 120 W, the number of carbocations generated in the solution precursor is limited. Therefore, there are not enough carbocations to reduce bismuth oxide to metallic bismuth. The final products at these experimental conditions are bismuth hydroxide at

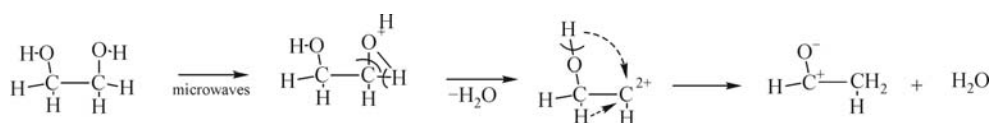


Fig. 9 The first stage of the chemical reaction.

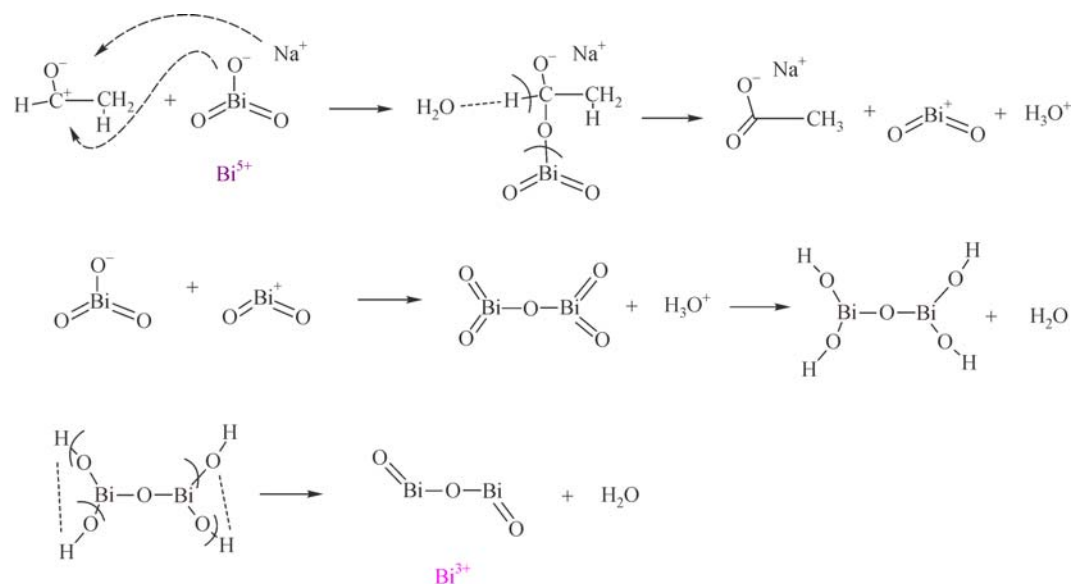


Fig. 10 The reduction mechanism to obtain bismuth oxide.

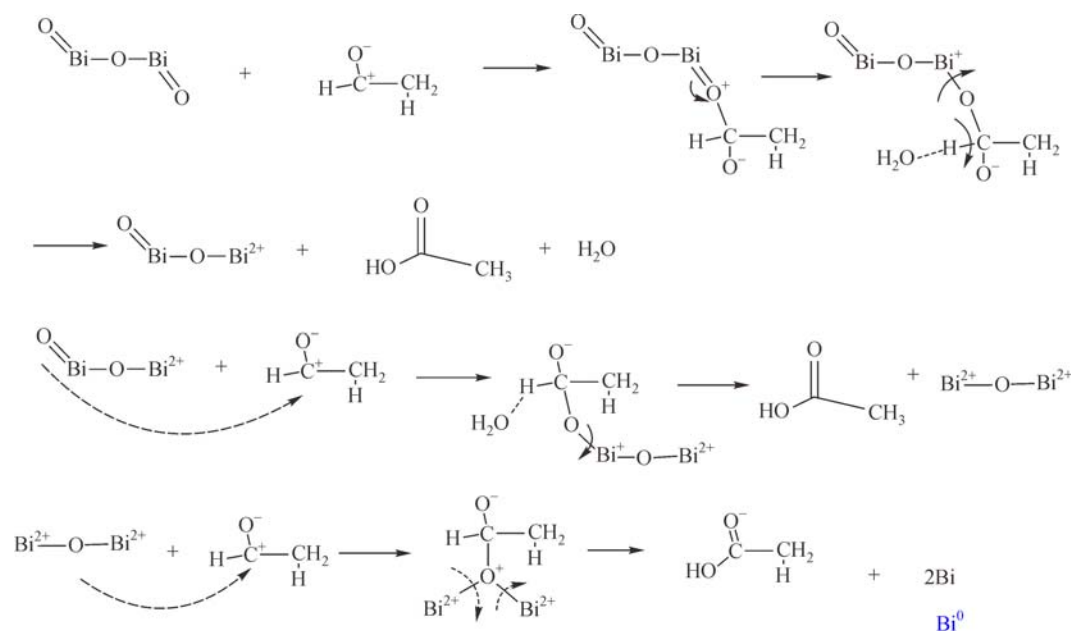


Fig. 11 The reduction mechanism to obtain metallic bismuth.

low concentration of the precursor solution (0.01 mol/L) and bismuth oxide flakes at a concentration of 0.03 and 0.05 mol/L.

4 Conclusions

Metallic bismuth micrometric spheres from 45 nm to 10 μm were obtained by a microwave-assisted solvothermal method at 600 and 1200 W with a 2.64 GHz. This was

an easy, economic, efficient and ecologic approach to generate metallic spheres because it allows a rapid crystallization due to the fact it generates a uniform heating of the reaction mixture with the creation of hot spots. At 600 W, the size of the bismuth spheres strongly depends on the concentration of the precursor solution. At lower concentration (0.01 mol/L), the average size of the spheres is in the order of 500 nm, while the size is increased to 1–5 μm if the solution precursor is supersaturated (0.05 mol/L). At higher power level, 1200 W, the situation

changes. If the power level is increased, the temperature of the vessel is also increased as well as the pressure of the container. The pressure of the system also depends on the concentration of the solution, therefore, a high pressure and temperature in a supersaturated solution generates the conditions to inhibit the growth process of the spheres. The average size in this case is in the order from 500 nm to 1 μm .

To conclude, the microwave power level controls the phase of the product. At high power level (600 and 1200 W), metallic bismuth micro-spheres are formed, while at a lower power level (120 W), 5 μm flake-like structures of bismuth oxide were acquired as an intermediary product. The necessary synthesis conditions were determined for the reactants, sodium bismuthate and ethylene glycol to obtain the reduction of Bi^{5+} and Bi^{3+} to Bi^0 .

Acknowledgements The authors of this article are grateful to Iván Puente and Alina Rendón for sample characterization by SEM and Andrea Santiago for reviewing this work. We also thank PAPIIT for its support by the research project (IN113411) and CONACYT for the PhD scholarship.

References

- [1] Wu J, Yang H, Li H, et al. Microwave synthesis of bismuth nanospheres using bismuthcitrate as a precursor. *Journal of Alloys and Compounds*, 2010, 498(2): L8–L11
- [2] Kharissova O V, Osorio M. Morphological studies of bismuth nanostructures prepared by hydrothermal microwave heating. *MRS Online Proceeding Library*, 2012, 1449: bb03-02
- [3] Liu X, Cao H, Yin J. Generation and photocatalytic activities of $\text{Bi@Bi}_2\text{O}_3$ microspheres. *Nano Research*, 2011, 4(5): 470–482
- [4] Huang Q, Zhang S, Cai C, et al. β - and α - Bi_2O_3 nanoparticles synthesized via microwave-assisted method and their photocatalytic activity towards the degradation of rhodamine B. *Materials Letters*, 2011, 65(6): 988–990
- [5] Bartonickova E, Cihlar J, Castkova K. Microwave-assisted synthesis of bismuth oxide. *Processing and Application of Ceramics*, 2007, 1(1–2): 29–33
- [6] Anandan S, Wu J J. Microwave assisted rapid synthesis of Bi_2O_3 short nanorods. *Materials Letters*, 2009, 63(27): 2387–2389
- [7] Ma M G, Zhu J F, Sun R C, et al. Microwave-assisted synthesis of hierarchical Bi_2O_3 spheres assembled from nanosheets with pore structure. *Materials Letters*, 2010, 64(13): 1524–1527
- [8] Jhung S H, Lee J H, Yoon J W, et al. Microwave synthesis of chromium terephthalate MIL-101 and its benzene sorption ability. *Advanced Materials*, 2007, 19(1): 121–124
- [9] Zhu H, Wang X, Li Y, et al. Microwave synthesis of fluorescent carbon nanoparticles with electrochemiluminescence properties. *Chemical Communications*, 2009, 34(34): 5118–5120
- [10] Wang X, Qu K, Xu B, et al. Microwave assisted one-step green synthesis of cell-permeable multicolor photoluminescent carbon dots without surface passivation reagents. *Journal of Materials Chemistry*, 2011, 21(8): 2445–2450
- [11] Panda A B, Glaspell G, El-Shall M S. Microwave synthesis of highly aligned ultra narrow semiconductor rods and wires. *Journal of the American Chemical Society*, 2006, 128(9): 2790–2791
- [12] Tompsett G A, Conner W C, Yngvesson K S. Microwave synthesis of nanoporous materials. *ChemPhysChem*, 2006, 7(2): 296–319
- [13] Borja-Urby R, Diaz-Torres L A, Garcia-Martinez I, et al. Crystalline and narrow band gap semiconductor BaZrO_3 : Bi–Si synthesized by microwave-hydrothermal synthesis. *Catalysis Today*, 2015, 250: 95–101
- [14] Knochel P, Molander G A, eds. *Comprehensive Organic Synthesis*. 2nd ed. Oxford: Elsevier, 2014, 237–239
- [15] Kappe C O. Speeding up solid-phase chemistry by microwave irradiation: A tool for high-throughput synthesis. *American Laboratory*, 2001, 33(10): 13–19
- [16] Sutton W H. Microwave processing of ceramic materials. *American Ceramic Society Bulletin*, 1989, 68: 376–386
- [17] Thostenson E T, Chou T W. *Microwave processing: Fundamentals and applications*. Composites Part A: Applied Science and Manufacturing, 1999, 30(9): 1055–1071
- [18] Zhu Y J, Chen F. Microwave-assisted preparation of inorganic nanostructures in liquid phase. *Chemical Reviews*, 2014, 114(12): 6462–6555
- [19] Leadbeater N E, ed. *Microwave Heating as A Tool for Sustainable Chemistry*. CRC Press, 2010, 6–9
- [20] Hayes B. *Microwave Synthesis Chemistry at Speed of Light*. USA: CEM Publishing, 2002, 14–16
- [21] Chandra U. *Microwave Heating*. Croatia: InTech, 2011, 3
- [22] Kappe C O, Dallinger D, Murphree S S. *Practical Microwave Synthesis for Organic Chemist, Strategies, Instruments and Protocols*. Wiley-VCH, 2009, 11–15
- [23] Hasegawa Y, Murata M, Nakamura D, et al. Thermoelectric properties of bismuth micro/nanowire array elements pressured into a quartz template mold. *Journal of Electronic Materials*, 2009, 38(7): 944–949
- [24] Dresselhaus M S, Dresselhaus G, Sun X, et al. Low-dimensional thermoelectric materials. *Physics of the Solid State*, 1999, 41(5): 679–682
- [25] Boukai A, Xu K, Heath J R. Size-dependent transport and thermoelectric properties of individual polycrystalline bismuth nanowires. *Advanced Materials*, 2006, 18(7): 864–869
- [26] Zhao X B, Ji X H, Zhang Y H, et al. Bismuth telluride nanotubes

- and the effects on the thermoelectric properties of nanotube-containing nanocomposites. *Applied Physics Letters*, 2005, 86(6): 062111
- [27] Zhou J, Jin C, Seol J H, et al. Thermoelectric properties of individual electrodeposited bismuth telluride nanowires. *Applied Physics Letters*, 2005, 87(13): 133109
- [28] Poudel B, Hao Q, Ma Y, et al. High-thermoelectric performance of nanostructured bismuth antimony telluride bulk alloys. *Science*, 2008, 320(5876): 634–638
- [29] Mishra S K, Satpathy S, Jepsen O. Electronic structure and thermoelectric properties of bismuth telluride and bismuth selenide. *Journal of Physics: Condensed Matter*, 1997, 9(2): 461–470
- [30] Maeder T. Review of Bi_2O_3 based glasses for electronics and related applications. *International Materials Reviews*, 2013, 58(1): 3–40
- [31] Aviv H, Bartling S, Grinberg I, et al. Synthesis and characterization of Bi_2O_3 /HSA core-shell nanoparticles for X-ray imaging applications. *Journal of Biomedical Materials Research Part B*, 2013, 101B(1): 101–138
- [32] Abdullah A H, Ali N M, Ibrahim M, et al. Synthesis of bismuth vanadate as visible-light photocatalyst. *The Malaysian Journal of Analytical Sciences*, 2009, 13(2): 151–157
- [33] Brezesinski K, Ostermann R, Hartmann P, et al. Exceptional photocatalytic activity of ordered mesoporous $\beta\text{-Bi}_2\text{O}_3$ thin films and electrospun nanofiber. *Chemistry of Materials*, 2010, 22(10): 3079–3085
- [34] Salvador J A, Silvestre S M, Pinto R M. Bismuth(III) reagents in steroid and terpene chemistry. *Molecules*, 2011, 16(4): 2884–2913
- [35] Lockner J. Bismuth in organic synthesis. *Bulletin of the Chemical Society of Japan*, 1996, 2673
- [36] Liao H, Nehl C L, Hafner J H. Biomedical applications of plasmon resonant metal nanoparticles. *Nanomedicine*, 2006, 1(2): 201–208
- [37] Lin D J, Huang H L, Hsu J T, et al. Surface characterization of bismuth-doped anodized titanium. *Journal of Medical and Biological Engineering*, 2013, 33(6): 538–544
- [38] Hernandez-Delgadillo R, Badireddy A R, Zaragoza-Magaña V, et al. Effect of lipophilic bismuth nanoparticles on erythrocytes. *Journal of Nanomaterials*, 2015, 264024 (9 pages)
- [39] Brown A L, Goforth A M. pH-Dependent synthesis and stability of aqueous, elemental bismuth glyconanoparticle colloids: Potentially biocompatible X-ray contrast agents. *Chemistry of Materials*, 2012, 24(9): 1599–1605
- [40] Rieznicenko L S, Gruzina T G, Dybkova S M, et al. Investigation of bismuth nanoparticles antimicrobial activity against high pathogen microorganisms. *American Journal of Bioterrorism, Biosecurity and Biodefense*, 2015, 2(1): 1004
- [41] Gong J, Lee C S, Chang Y Y, et al. A novel self-assembling nanoparticle of Ag–Bi with high reactive efficiency. *Chemical Communications*, 2014, 50(62): 8597–8600
- [42] Valverde-Aguilar G, Prado-Prone G, Vergara-Aragón P, et al. Photoconductivity studies on nanoporous TiO_2 /dopamine films prepared by sol-gel method. *Applied Physics A*, 2014, 116(3): 1075–1084
- [43] Boeré R T, Duke M. *Chemistry 2810 Laboratory Manual*. Springer, 2003, 1–22
- [44] Wang Y, Zhao J, Zhao X, et al. A facile water-based process for preparation of stabilized Bi nanoparticles. *Materials Research Bulletin*, 2009, 44(1): 220–223
- [45] Wang J, Wang X, Peng Q, et al. Synthesis and characterization of bismuth single-crystalline nanowires and nanospheres. *Inorganic Chemistry*, 2004, 43(23): 7552–7556